



However, it is difficult and ambiguous to decide whether Fig. 2(b) is of low quality or of high quality. For the second row, when asked to choose their favorite image, some of our respondents preferred Fig. 2(e) to Fig. 2(d) while other users reported the opposite choice, since aesthetics is highly subjective and complex – each user has his or her own judgment of what is beautiful.

Recently, instead of using traditional hand-crafted low level features, the state-of-art feature extraction technique based on deep learning has been involved to evaluate the aesthetic quality of images [14, 15, 18, 32]. Compared with those traditional methods, the most notable difference is that the deep features of the input images could be extracted automatically without making any artificial approximations of the aesthetic rules. However, most of above work pay their attention on the task of high accuracy binary classification without considering the subjectivity and personal preference of diverse individuals. In [29], Ren et al. try to address this personalized aesthetics problem by showing that individual’s aesthetic preferences exhibit strong correlations with content and aesthetic attributes, and the deviation of individual’s perception from generic image aesthetics is predictable. They propose a new approach to personalized aesthetics learning that can be trained even with a small set of annotated images from one user. However, since one user’s preference is highly subjective and his/her choice one time is occasional, a small set of annotated images is insufficient to fully represent his or her personal preference.

To solve the above problems, in this paper, we propose a novel and interactive user-friendly aesthetic ranking framework, called User-specific Aesthetic Ranking (USAR), which consists of three modules: primary personalized ranking (PPR), interaction stage (IS) and user-specific aesthetic distribution (USAD). The proposed framework takes as input a series of photos that users prefer, and produces as output a reliable, user-specific aesthetic distribution matching with users’ preference. In the module of PPR, an unique and exclusive dataset will be constructed interactively to describe the preference of diverse individuals by retrieving the most visually-similar images with regard to those specified by users. This is based on the fact that the aesthetic preference of one user will remain unchanged for a long time [4, 29]. The powerful Deep Convolutional Neural Network is involved and optimized to retrieve those content similar images through several amount of interactions in the module of IS. Based on this unique user-specific dataset and sufficient well-designed aesthetic attributes, a customized aesthetic distribution model will be learned in the module of USAD, which concatenate both personalized preference and photography rules. Given an input image, its corresponding aesthetic distribution will be computed by USAD. After that, the correlation coefficient between one user’s specific aesthetic distribution and that of input image can be obtained. The larger the coefficient is, the higher aesthetic score and ranking is. We conduct extensive experiments and user studies on two large-scale public datasets, and demonstrate that our framework outperforms those work based on conventional aesthetic assessment or ranking model.

The contributions of this paper mainly focus on the following three fold:

- We propose a novel and user-friendly aesthetic ranking framework via powerful deep neural network and small

amount of interaction to automatically rank the aesthetic quality of images in accordance with users’ preference.

- We propose an efficient and limited interactive method to construct an unique and exclusive dataset to represent the aesthetic preference of diverse individuals, which can overcome the problem of users’ subjective preference and occasional choice.
- We propose a customized aesthetic distribution model based on an unique user-specific dataset and sufficient well-designed aesthetic attributes, which concatenate both users’ personalized preference and photography rules.

## 2 RELATED WORK

User-specific aesthetic quality ranking mainly concerns two important problems: how to evaluate the aesthetic quality of images and how to collect user-specific images. In this section, we first review related aesthetic quality assessment work, then discuss the problem concerning personalized searching and ranking, which is used to collect user-specific images.

Most existing research works have focused on hand-crafted visual features that all high-quality images share. Extensive experiments have been conducted with both low level visual features [2, 5, 21, 25] and high-level features combinations [3, 7, 13, 16, 20, 24, 26, 30, 31, 34]. Datta et al. [5] focused their attention on utilizing a computational approach to understand images using a 56-dimensional features vector. Luo et al. [21] first proposed subject region extraction on the assumption that professional photographers focus on their subjects while blurring the background. Mavridaki et al. [25] proposed the use of aesthetic feature pattern, coupled with other features such as simplicity, sharpness, composition etc. Aydin et al. [2] presented five features (sharpness, colorfulness, tone, clarity, depth) to measure the image quality to enable automatic analysis and editing. Not satisfied with the results of low level visual features, some researchers have turned their attention to the combination of high level features. Dhar et al. [7] proposed high level describable attributes based on content, composition and sky illumination to predict the interestingness of the input images. Lo et al. [16] proposed a set of features that are discriminative, and computationally efficient without adopting any computationally intensive techniques. Luo et al. [20] extracted different features for different categories of photos and then generate category-specific classifiers. Although hand-crafted features play a certain role in assessing the image quality, it is a man-made approximation of the abstract aesthetic rules and might fail to capture the full diversity and beauty of a photographic image.

In recent years, with the rise of deep learning, the extraction of deep features have gradually become popular for the task of image quality assessment. Lu et al. [18] developed a double-columned deep convolutional neural network to capture both global and local characteristics of images. Dong et al. [20] directly utilized a model trained on ImageNet [15], acquiring a 4096 dimensions feature vector extracted from the former and achieved a better performance. Tian et al. [32] focused on the similarity of images in the same category to propose a query dependent model consisting of both deep visual features and semantic features. Despite the high accuracy of the binary classification tasks that deep neural network achieves,

USAR: an interactive user-specific aesthetic ranking framework for images



**Figure 2: (Top row) The constraints of the conventional binary classification. (a) is deemed as low quality while (c) scores much higher. It is difficult to quantify the actual quality of (b). (Bottom row) Personal preference varies between different individuals. One of our attendants prefers human portraits in (d) while another one likes lightning images in (e).**

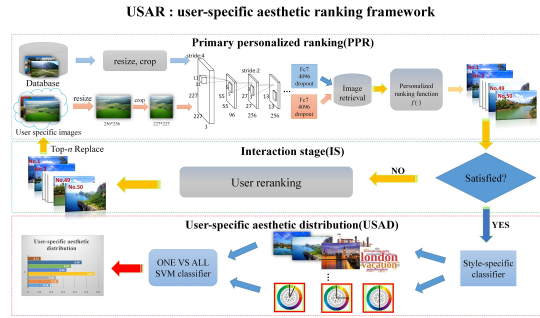


**Figure 3: The overview of our user-specific aesthetic ranking framework. The framework consists of three modules: Primary personalized ranking(PPR), Interaction stage(IS) and User-specific aesthetic distribution(USAD).The PPR is applied to construct an unique and exclusive dataset to represent the aesthetic preference of diverse individual. The IS is deployed to refine the AlexNet as well as the PPR. Finally, the images ranked by PPR is sent to USAD to generate the user-specific aesthetic distribution.**

it can not extract the meaning of aesthetics in the absolute sense and can not understand personal preference. Ren et al. [29] try to address this personalized aesthetics problem by showing that individual’s aesthetic preferences exhibit strong correlations with content and aesthetic attributes, and the deviation of individual’s perception from generic image aesthetics is predictable. They propose a new approach to personalized aesthetics learning that can be trained even with a small set of annotated images from a user.

Our proposed User-specific Aesthetic Ranking (USAR) framework tries to address above problems. To overcome the shortcomings of low or high level visual features, a powerful and iterative optimized AlexNet is deployed to capture the full diversity of user selected images. Aiming at the problem of unstable personalized ranking of images, we try to construct an unique and exclusive dataset with users’ interactions. Based on the unique user-specific dataset and sufficient well-designed aesthetic attributes, a customized aesthetic distribution model is learned, which concatenates both personalized preference and photography rules.

### 3 USER-SPECIFIC AESTHETIC RANKING FRAMEWORK

In this paper, we propose a user-specific aesthetic ranking framework by using a massive image database via AlexNet (illustrated in Fig. 3). which consists of three modules: 1) Primary personalized ranking, 2) Interaction stage and 3) User-specific aesthetic ranking. Given a set of preferred images  $U$ , we first extract their content features for further retrieval of similar images from the whole aesthetic database  $\Gamma$  and construct a retrieval set  $S(I_i)$ . Then a primary personalized ranking  $R_{PPR}$  is generated from the primary personalized ranking module. In order to overcome the instability suffered from the directly use of a small amount of fsample, i.e., the user-specific image, we perform refining strategy by asking user to interact with the primary ranking image and treat it as the ground-truth, which is subsequently sent to our style-specific classifier to generate a user-specific aesthetic distribution  $D_{USAR}$ . During the testing stages, the learned ranking module outputs the testing distribution  $D_{test}$ . Consequently, user-specific aesthetic ranking is obtained by calculating the correlation coefficients between  $D_{USAR}$  and  $D_{test}$ .

### 3.1 Primary Personalized ranking

Due to the strong representability of the deep feature, we deploy Deep Convolutional Neural Network to understand images. The features we extracted are based on AlexNet used in ImageNet proposed and designed by Krizhevsky et al. [15]. As for the extraction on feature of aesthetic attributes, there is no need to construct excessively network. AlexNet is well-matched for the requirement on extracting aesthetic feature as well as time while we refine the whole network to generate user-specific aesthetic model. Take a glance at Fig. 3, we first ask user to pick  $m$  images that they prefer, denoted by user-specific images. Then the image retrieval method described below is applied to learn a customized ranking function outputting primary personalized ranking. We adopt the interaction strategy by requiring user to rerank the top  $n$  image and replace it with the original user-specific image. This aims at refining the whole AlexNet by reranking user's ranking to fit the personalized choice. The work flow detailed above will iterate  $N$  times in an attempt to get the ideal fitting results.

Let us turn to the image retrieval method adopted. Suppose  $U = \{I_{u1}, I_{u2}, \dots, I_{un}\}$  be the set of preferred images that user chooses where  $I_u$  denotes the most beloved image of the user and sanctify  $U \in \Gamma$ , where  $\Gamma$  is the entire aesthetic database. For a given image  $I_u$ , we first extract its visual features for the retrieval of the similar images from  $\Gamma$ . For the retrieval purpose, we aim to explore the neighbors of the user-specific image in a joint visual space by adopting the equation below:

$$S^{(I_i)} = \{I_i, I_i \in \Gamma \cap I_i \in \Psi\} \quad (1)$$

where  $\Psi$  is neighboring joint visual space of user-specific image. For every user-specific image, we perform different strategy, dynamically select  $m$  similar images that are retrieving from  $\Gamma$  and concatenate the images into a retrieval result  $S^{(I_i)}$ . Once the retrieval result is obtained, a user-specific ranking function  $f(\cdot)$  is learned to predict the level of  $I_u$ .

As soon as the personalized retrieval result  $S^{(I_i)}$  is generated, the objective of our model is to predict user's preference with a new testing image inputs. We are given a aesthetic database  $\Gamma = \{I_i\}, i = 1, 2, 3, \dots, n$ , which is represented by the feature vector  $\{x_i\} = \{x_1, x_2, \dots, x_n\}$ , where  $n$  denotes the dimension of the features extracted from the deep network.

The goal of our USAR model is to learn a personalized ranking function shown as follow:

$$r(x_i) = w^T x_i \quad (2)$$

so it can be maximized to satisfied the following constraints :

$$\forall (i, j) \in \Gamma : w^T x_i > w^T x_j \quad (3)$$

This approach is similar to that used in SVM classification, where the goal is to generate a relative image pair in accordance with the query identification within. This leads to an optimization problem shown as below:

$$\begin{aligned} \min & \left( \frac{1}{2} \|w^T\|_2^2 + C(\sum \xi_{ij}) \right) \\ \text{s.t.} & w^T x_i - w^T x_j \geq 1 - \xi_{ij}; \forall (i, j) \in \Gamma \\ & \xi_{ij} \geq 0 \end{aligned} \quad (4)$$

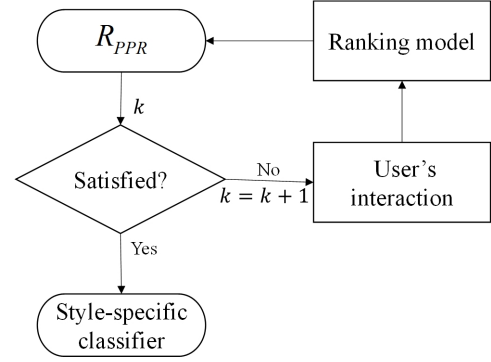


**Figure 4: The pipeline of the IS.** After acquiring the  $R_{PPR}$ , interaction stage is applied to refine the ranking model with user's interaction. If users are satisfied with the  $R_{PPR}$ , we then send the images in  $R_{PPR}$  to style-specific classifiers. If not, users are allowed to implement a series of operation such as rerank or delete. The top- $n$  of the new  $R_{PPR}$  is sent to replace the user-specific images for the refinement of the PPR

Where  $w$  is weight vector on ranking function,  $C$  is tradeoff between training error and margin.  $\xi_{ij}$  is slack variable of different image pairs. We solve this problem by training a linear kernel with  $SVM^{rank}$  [11]. We denote the primary personalized ranking released by the ranking function as  $R_{PPR}$ .

### 3.2 Interaction stage

Considering the probable instability suffered from small sample directly use of user-specific image, we propose refinement strategy by adding user's interaction on  $R_{PPR}$ . We first ask user to interact with our system by reranking  $R_{PPR}$   $k$  times and treat the new  $R_{PPR}$  denoted by  $R_{UPPR}$  as the prior ground truth data of the user. The concrete workflow is shown in Fig. 4 as follow:

Specifically, after generating the  $R_{PPR}$ , users are required to rerank the  $R_{PPR}$ . We dynamically adjust the reranking times  $k$  in accordance with user's interaction, say, we set  $k$  at 0 if user are satisfied with the  $R_{PPR}$ . Otherwise, the reranked  $R_{PPR}$  is sent to *Primary Personalized ranking generation* stage to regenerate the new  $R_{PPR}$  denoted by  $R_{UPPR}$  and  $k$  is updated accordingly. Since our goal is to accurately explore and localize the user's preference, we test the performance of  $R_{UPPR}$  by selecting different  $k$ . Finally, it is send to generate a user-specific aesthetic distribution  $D_{USAR}$ .

### 3.3 User-specific aesthetic distribution generation

After acquiring the primary personalized ranking, we turn to focus on the user-specific aesthetic ranking that combine with both aesthetic rules and user's preference. Being aware of that primary personalized ranking is learned latently from user-specific image and hasn't dug deep on why the user show preference in certain kind of images, we propose a well-designed style-specific aesthetic attribute classifier. Specifically, we investigate the high quality images both on professional photographic websites and the social network



**Table 1: The chosen aesthetic attributes**

| Aesthetic attribute  | Method | Aesthetic attribute | Method |
|----------------------|--------|---------------------|--------|
| Rule of Thirds       | [25]   | Tone                | [7]    |
| Center composition   | [25]   | Use of light        | [20]   |
| HROT                 | [25]   | Saturation          | [5]    |
| Sharpness            | [25]   | Image size          | [28]   |
| Pattern              | [25]   | Edge Composition    | [28]   |
| Complementary Colors | [20]   | Global Texture      | [16]   |
| Subordinate Colors   | [20]   | SDE                 | [13]   |
| Cooperate Colors     | [20]   | Hue count           | [13]   |
| Complexity feature   | [20]   | Depth of field      | [7]    |

and find that visually pleasing images always share certain aesthetic rules. Inspired by the task of multi-label classification, we proceed to generate a aesthetic distribution that integrate dozens of aesthetic attributes for every input image in the primary personalized ranking. Then, by concatenating distribution of each image in the  $R_{UPPR}$ , a final aesthetic distribution of the user is released. In this part, we try to describe each ranking image via a set of well-designed aesthetic attributes. Therefore, we present dozens of representative aesthetic feature that are commonly used in photography and construct a style-specific classifier. The aesthetic attribute we adopt are listed in Table 1 as follow:

With the feature of elaborate aesthetic attribute generated with the aforementioned extracting stage, each input image with several sets of label is sent to our pre-trained one vs all classifier to generate a style-specific aesthetic distribution. The user-specific aesthetic distribution  $D_{USAR}$  is calculated by concatenating all the single style-specific distribution as defined below:

$$D_{USAR} = \sum_{i=1}^C \frac{r_C - i + 1}{r_C \sum C} a_i \quad (5)$$

In the equation above,  $r_C$  is the ranking of  $C$ -th image's distribution. And  $a_i$  represents aesthetic score of  $i$ -th set.

Since the user-specific aesthetic distribution is established from primary ranking and multi-aesthetic attribute, there is no need to apply any internal strategies for capturing user's preference. Moreover, due to the learning of customized hyperplane, our framework avoids the instability suffered from the direct learning of user-specific image and enable a insightful and effective ranking. We adopt strategy shown below to generate user-specific aesthetic ranking:

$$S = \frac{(D_{USAR} - \overline{D_{USAR}}) \sum_{i=1}^n (D_{test} - \overline{D_{test}})}{\sqrt{(D_{USAR} - \overline{D_{USAR}})^2} \sqrt{\sum_{i=1}^n (D_{test} - \overline{D_{test}})^2}} \quad (6)$$

where  $D_{test}$  indicates the distribution of testing image,  $S$  represents the relative score between  $D_{USAR}$  and  $D_{test}$ .

### 3.4 Testing stage

After the user-specific aesthetic ranking (USAR) framework is learned during the training stage, we proceed to test our model as

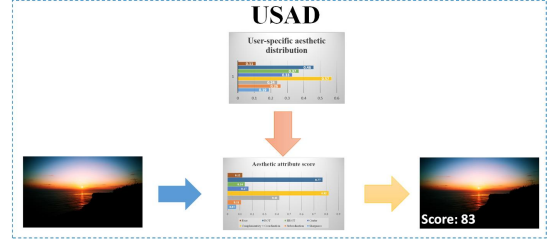


**Figure 5: The workflow during testing stage.** For a given testing image, we send it to style-specific classifier to generate a testing aesthetic distribution  $D_{test}$ . Then, a score is deduced by calculating the correlation between testing distribution  $D_{test}$  and user-specific aesthetic distribution  $D_{USAR}$

show in Fig. 5. Given a set of images to be tested, we conduct the following two tasks in parallel: 1) for user-specific images, we use our unique model to generate the relative rankings with real value scores. Specifically, for a given testing image, we send it to style-specific classifier to generate testing distribution  $D_{test}$ . Then, a real-valued score is deduced by calculating the correlation between  $D_{test}$  and  $D_{USAR}$ . 2) we also send the images to the respondents, who were required to view and rate the same testing images as depicted in task 1. We use these respondent-generated scores as the ground truth in our experiment. Finally, we compare our prediction results with the ground truth to verify the effectiveness of our proposed model.

## 4 EXPERIMENTS

In this section, we introduce how we conduct the experiment on two large scale public datasets and the comparison with other state-of-art methods.

### 4.1 Dataset

The AVA dataset is a new large-scale dataset for conducting aesthetic visual analysis, which was collected by Murray et al. [23]. It contains over 250,000 images along with a rich variety of meta-data including a large number of aesthetic scores for each image collected during the digital photography contest on dpchallenge.com [9]. Each image on the website is commented and scored by users, commenter, participants and non-participants and the average score is provided. We treat the image with an average score of 5 plus as high quality and 5 minor as low quality as detailed in [22]. For the purpose of minimized error, we randomly split the data ten times and assign half of them to training and the rest to the testing set.

The FLICKR-AES dataset is constructed by 40000 photos with their aesthetic ratings marked by AMT downloaded from Flickr [10]. The aesthetic ratings range from the lowest 1 to the highest 5 to demonstrate the different aesthetic level. Each image in dataset is evaluated by five different AMT workers participated in annotation work of FLICKR-AES.

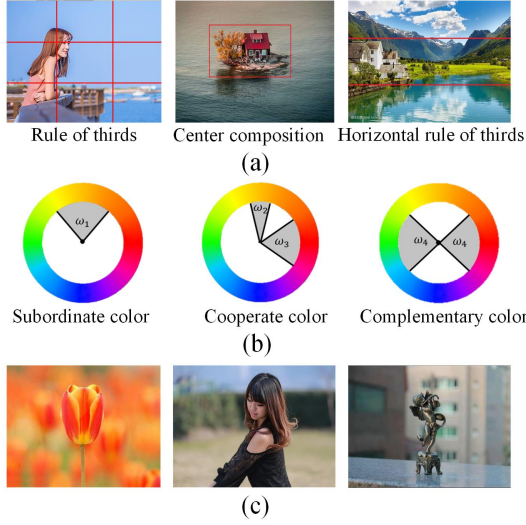


**Figure 6: Part of the metric images containing aesthetic attribute for users to refer to while annotating their personal ground-truth**

## 4.2 Experimental setting and Method comparison

To validate the effectiveness of our user-specific aesthetic ranking learned with user's preference and  $D_{USAR}$ , we first compare the results with those of several state-of-arts personalized aesthetic assessment method PAM [29], FPMF [1], [28], and [6] that are proposed in recent years .

**4.2.1 Comparison with other methods.** For comparison with PAM and FPMF, we conduct experiments with the same experimental setting on FLIKR-AES dataset. The averaged results as well as the standard deviation is reported. To evaluate the performance on AVA image dataset, we compare the result of [14], [28] and [6] in terms of ranking correlation measured by Spearman's  $\rho$  between the estimated aesthetics scores and the ground-truth scores. Suppose  $r_k$  represents the  $k$ -th rank sorted by algorithm with the score  $S_k$  and  $\hat{r}_k$  indicate the rank when ordered by user with the score  $\hat{S}_k$ . Subsequently,  $d_k = r_k - \hat{r}_k$  is then substituted to  $\rho = 1 - \frac{6 \sum d_k^2}{n^3 - n}$  measuring the discrepancy between two ranks. The  $n$  represents the number of the images. The coefficient  $\rho$  lies in range within  $[-1, 1]$ .

**4.2.2 USAR with different setting.** To thoroughly study and compare the various user-specific aesthetic ranking method, we implement three methods and compare them with each other:

**USAR\_PPR :** In our user-specific aesthetic model, we first generate the  $R_{PPR}$  by learned customized ranking function  $f(\cdot)$ . Generally, we acquire the user's preference by latently import preferred image to the system and we denote the model as USAR\_PPR for short.

**USAR\_PAD:** For comparison with USAR\_PPR, we choose to directly use user-specific image as input to generate a concatenated aesthetic attribute distribution. For each testing image  $I_t$ , we send

**Table 2: Performance of our algorithm compared to other methods in FLICKR-AES Dataset**

|                              | 10images                            | 100images                           |
|------------------------------|-------------------------------------|-------------------------------------|
| FPMF (only attribute)        | $-0.003 \pm 0.004$                  | $0.002 \pm 0.003$                   |
| FPMF (only content)          | $-0.002 \pm 0.002$                  | $0.002 \pm 0.01$                    |
| FPMF (content and attribute) | $-0.001 \pm 0.003$                  | $0.01 \pm 0.007$                    |
| PAM (only attribute)         | $0.004 \pm 0.003$                   | $0.025 \pm 0.013$                   |
| PAM (only content)           | $0.001 \pm 0.004$                   | $0.021 \pm 0.017$                   |
| PAM (content and attribute)  | $0.006 \pm 0.003$                   | $0.039 \pm 0.012$                   |
| USAR_PPR                     | $0.003 \pm 0.002$                   | $0.026 \pm 0.007$                   |
| USAR_PAD                     | $0.002 \pm 0.003$                   | $0.019 \pm 0.003$                   |
| <b>USAR_PPR&amp;PAD</b>      | <b><math>0.007 \pm 0.004</math></b> | <b><math>0.034 \pm 0.015</math></b> |

it directly to style-specific classifier and obtain a  $D_{test}$ . We generate the relative ranking by simply calculating its correlation and normalize it into certain range. The model above is marked by USAR\_DAP for short.

**USAR\_PPR&PAD:** The objective of our proposed framework is to interactively generate a reliable user-specific aesthetic distribution. To achieve this, we organically concatenate the USAR\_PPR and USAR\_PAD with user's interaction involving. Specifically, given a set of images  $U_{test} = (I_{t1}, I_{t2}, \dots, I_{ti})$  to be assessed, we conduct the experiments shown as follow. The proposed framework first randomly select several images from the  $\Gamma$  and present them to the users. By choosing several user-specific images, a primary personalized ranking  $R_{PPR}$  is enforced by learned customized hyper plane. Considering the instability caused by small sample, we apply the interactive strategy detailed in *Primary personalized ranking generation* and ask user to rerank the  $R_{PPR}$  to acquire a new  $R_{PPR}$  denoted by  $R_{NPPR}$ . Then we ask our respondents to view all the images of the testing dataset and rank the testing images in accordance with their preference. This is treated as the ground truth for our personalized ranking system. Meanwhile, the same testing images are sent to our proposed framework to generate a user-specific ranking  $R_{USAR}$ .

The comparison described above only involve the vertical comparison with different experimental setting. To validate the robustness of our proposed user-specific aesthetic distribution  $D_{USAR}$ , we implement the experiments 50 times on measuring the stability of the  $D_{USAR}$  and present the correlation between  $D_{USAR}$  and ground truth distribution  $D_{GTD}$ .

As for the ground-truth, we acquire the ground-truth ranking and distribution by inviting 20 users to participate in our test. All the user are required to rank the testing image in accordance with their preference. For the generation of the benchmark distribution, we ask user to annotate the certain aesthetic label with the benchmark metric shown in 6. For each user, we collect 50 set of benchmark ranking and distribution marked by  $R_{GTR}$  and  $D_{GTD}$  and use it for measuring the performance with the different setting.

## 4.3 Result and discussion on FLICKR-AES dataset

In this section, we compare our results with those of FPMF and PAM to verify the effectiveness of the proposed algorithm. The averaged

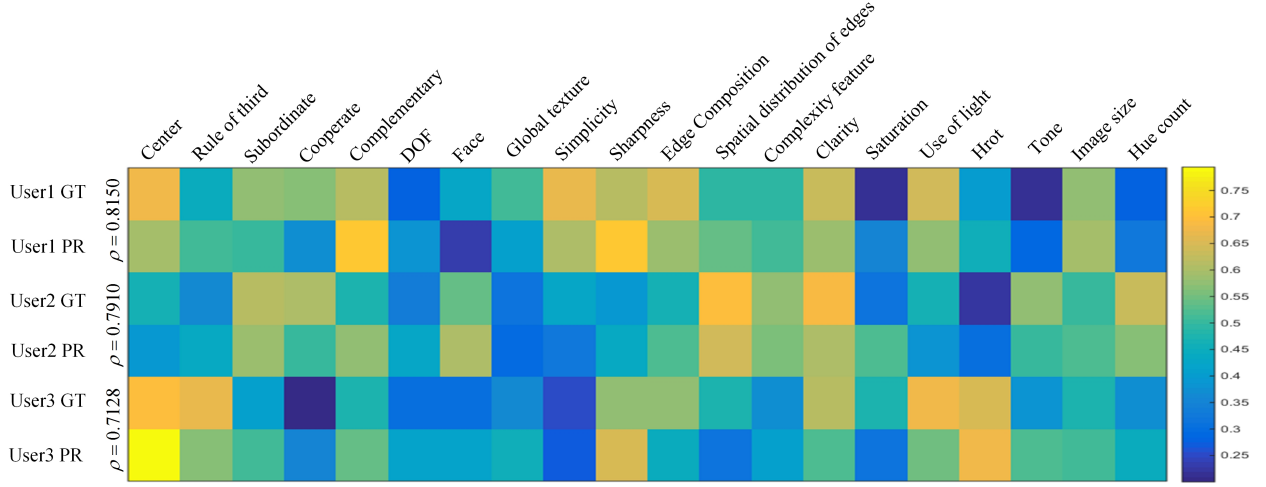


Figure 7: The correlation between ground-truth aesthetic distribution and prediction aesthetic distribution of users.

score as well as the standard deviation obtained on FLICKR-AES dataset with the number of 10 and 100 images is reported in Table 2. Obviously, our three USAR models (last row in Table 2) outperform the FPMF model well. We then focus on the comparison between PAM and USAR. The data in second column represents the metric while selecting 10 images, which is identical to selecting 10 user-specific images. As shown in Table 2, USAR\_PPR&PAD outperform the PAM(content and attribute) while  $m$  is at 10. Even compared with results of PAM while  $m$  is at 100, our USAR\_PPR&PAD still demonstrates a competitive performance with the averaged improvement of 0.034, which validate the design of our user-specific aesthetic ranking model, fully leverages the common understanding of multiple aesthetic attributes and user’s preference, and well focuses on the interaction with  $R_{UPPR}$  from the specific user.

We deem that excellent performance is achieved by two aspects: 1) USAR\_PPR initially learns the user’s preference by unique retrieval result that are similar to user-specific images. Then the user’s interaction enables a robust preference localization on stabilizing user’s preference. 2) The deployment of multiple aesthetic attributes enhance the performance initially deduced from  $R_{UPPR}$  and enforce the ideal style-specific preference of the user.

We also calculate the ranking correlation introduced above to measure the consistency between the prediction and ground-truth data. Compared with the  $\rho$  of 0.514 in [29], our mean ranking correlation over all the users are 0.518, which slightly outperform the former.

#### 4.4 Results and discussion on AVA dataset

The ranking correlation as well as accuracy on classification obtained on AVA Dataset are summarized in Table 3. Let us first compare the proposed USAR model with the AlexNet\_FT.Conf [14] and JR\_RSVM. The comparison indicates that our framework all significantly outperforms the AlexNet\_FT.Conf with a at least margin at 0.088, regardless of the different setting of the USAR. We then turn to the comparison with JR\_RSVM [28], Reg+Rank+Att+Cont [14]

Table 3: Performance of our algorithm compared to other methods in AVA Dataset

| Method                  | $\rho$        | ACC(%)       |
|-------------------------|---------------|--------------|
| Murray et al.           | -             | 68.00        |
| SPP                     | -             | 72.85        |
| RDCNN semantic          | -             | 75.42        |
| DMA_AlexNet_FT          | -             | 75.41        |
| JR_RSVM                 | 0.52          | -            |
| JR_RSVM                 | 0.30          | -            |
| AlexNet_FT_Conf         | 0.4807        | 71.52        |
| Reg+Rank+Att            | 0.5445        | 75.48        |
| Reg+Rank+Cont           | 0.5412        | 73.37        |
| Reg+Rank+Att+Cont       | 0.5581        | 77.33        |
| USAR_PPR                | 0.6002        | 72.41        |
| USAR_PAD                | 0.5446        | 77.69        |
| <b>USAR_PPR&amp;PAD</b> | <b>0.5687</b> | <b>77.98</b> |

and USAR. The bottom seven rows in Table 3 shows that proposed **USAR\_PPR&PAD** with the Primary personalized ranking refined by user’s interaction and Personalized aesthetic distribution yields the best performance (0.5687). Of the three models, the accuracy of USAR\_PPR (0.6002,72.41%) is slightly weaker on accuracy compared with that of Reg+Rank+Att (0.5445,75.48%) while ranking correlation  $\rho$  is much stronger than that of the latter (0.6002). Let us compare the results of USAR\_PAD, it is obvious that USAR\_PAD outperforms Reg+Rank+Cont with the margin on  $\rho$  and ACC(%) at 0.034 and 2.3. For the comparison with JR\_RSVM and Reg+Rank+Att+Cont, USAR\_PPR&PAD shows the relative better performance both on ranking correlation and accuracy at 0.5687 and 77.98. The performance above is under the setting of  $m$  and  $k$  at 5 and 3.

Since the coefficient  $\rho$  is calculated indirectly from the  $D_{USAR}$ , it is imperial to evaluate the performance  $D_{USAR}$ . We report the

**Table 4: Ranking correlation measured by  $\rho$  with different  $k$  and  $m$** 

| Interaction times(k) | The number of user-specific image(m) |        |        |
|----------------------|--------------------------------------|--------|--------|
|                      | 5                                    | 10     | 15     |
| 1                    | 0.4869                               | 0.4823 | 0.4431 |
| 2                    | 0.5341                               | 0.5389 | 0.5146 |
| 3                    | <b>0.5687</b>                        | 0.5684 | 0.5427 |
| 4                    | 0.5694                               | 0.5552 | 0.5345 |
| 5                    | 0.5776                               | 0.5761 | 0.5644 |

comparison between predicted distribution and the  $D_{GTD}$  as shown in Fig. 7. We list three of the 20 users and show the  $\rho$  between ground-truth distribution(GT) and personalized distribution(PR) respectively. The comparison result show the high correlation with the maximum  $\rho$  at 0.8150, which validate the effectiveness of the  $D_{USAR}$ .

We further explore whether or not the proposed USAR\_PPR&DAP is capable of stabilizing user's preference with the limited choice of  $m$  and  $k$ . To achieve this, we test the 20 users and calculate the ranking correlation  $\rho$  between the ground-truth ranking and each individual's ranking with the varying parameter of  $m$  and  $k$ . We then report performance in Table 4.

From the Table 4, we can see that proposed USAR\_PPR&DAP achieves the best performance with the  $\rho$  at 0.5687 when  $m$  and  $k$  are at 5 and 3, followed by 0.5776 with  $m = 5, k = 5$ . When compared with results on  $m = 10$  and  $m = 15$ , the performance on  $m = 5$  outperforms the majority counterparts, where the maximum margin has reached 0.0438( $m = 5, k = 1$  and  $m = 15, k = 1$ ). Even by increasing the interaction times  $k$ , the performance on  $m = 10$  and  $m = 15$  are still slightly weaker than that of  $m = 5$ . We expect this is due to two aspects: (1) The emphasis on selecting image while the number of user-specific image is limited. During the interaction stage, we observe our users and find that they tend to select the most beloved images while  $m$  is set relatively small, e.g.,  $m = 5$ . The majority of five chosen images are of high quality (at least for the user's opinion) or middle quality. This enables a robust learning to generate a reliable primary personalized ranking, the same to the user-specific aesthetic distribution. In contrast with the former, when  $m$  is set at 10 and more, user are inclined to pay more attention to the first several images. Specifically, the images ranked higher present the user's preference a bit more while that ranked lower present relatively less and mix the noise inevitably.

(2) The influence of different  $k$ . Throughout the whole result, the coefficient  $\rho$  is positively related with trend of  $k$ . However, it begin to decrease while users are choose 10 and 15 user-specific images with  $k = 4$ . We assume that the suddenly decrease suffers from the over interaction with  $R_{PPR}$ . For one part, the excessive interaction might cause the aesthetic fatigue. For another, it is impractical to conduct experiment with too much interaction involved.

Based on the aforementioned two reasons, we set  $m = 5, k = 3$  and compare our result on FLIKR-AES and AVA dataset as detailed above.

## 5 CONCLUSION AND FUTURE WORK

We propose a novel and user-specific aesthetic ranking model which first combines the results of deep neural net-work with individual preference to explore a new overlap between the subjective feeling of the users and the aesthetic abstract. In our proposed ranking framework, we construct a reliable ranking framework consisting of Primary personalized ranking, Interaction stage and User-specific aesthetic distribution. Experimental results on two large datasets demonstrate the effectiveness and efficiency of our approach in two aspects: 1) Our framework obtains a excellent performance on predicting user's preference, of which results are closer to the personal intention. 2) Our framework enable a robust user-specific aesthetic distribution on user's preference and achieve relative high correlation when compared with previous work. Although we have achieve excellent performance by unseeing Alexnet, which has a simpler structure, to extract image features. It still takes a while to interact with while we proceed to fine-tuning the network again. In the future work, it is imperial to speed up the refinement so that consuming time of interaction stage could be reduced. Besides, the extracted aesthetic features in style-specific classifier are still hand-crafted features. In the future work, we manage to deploy stronger feature representation by adopting more powerful network structure, setting unique convolutional kernel and combining both hand-crafted and deep aesthetic feature in an attempt to a more accurate user's personalized aesthetic preferences distribution.

## REFERENCES

- [1] Aseem Agarwala, Aseem Agarwala, and Aaron Hertzmann. 2014. Collaborative filtering of color aesthetics. In *The Workshop on Computational Aesthetics*. 33–40.
- [2] Tunc Ozan Aydin, Aljoscha Smolic, and Markus Gross. 2015. Automated Aesthetic Analysis of Photographic Images. *IEEE Transactions on Visualization and Computer Graphics* 21, 1 (2015), 31–42.
- [3] Subhabrata Bhattacharya, Rahul Sukthankar, and Mubarak Shah. 2010. A framework for photo-quality assessment and enhancement based on visual aesthetics. In *International Conference on Multimedia, Firenze, Italy, October*. 271–280.
- [4] M Cerf, D. R. Cleary, R. J. Peters, W. Einhuser, and C Koch. 2007. Observers are consistent when rating image conspicuity. *Vision Research* 47, 24 (2007), 3052–3060.
- [5] Ritendra Datta, Dhiraj Joshi, Jia Li, and James Z Wang. 2006. Studying aesthetics in photographic images using a computational approach. In *European Conference on Computer Vision, Graz, Austria, May*. 288–301.
- [6] Xiang Deng, Chaoran Cui, Huidi Fang, Xiushan Nie, and Yilong Yin. 2017. Personalized Image Aesthetics Assessment. In *ACM on Conference on Information and Knowledge Management*. 2043–2046.
- [7] S. Dhar, V. Ordonez, and T. L. Berg. 2011. High level describable attributes for predicting aesthetics and interestingness. In *IEEE Computer Society Conference on Computer Vision and Pattern Recognition, Colorado Springs, United states, June*. 1657–1664.
- [8] Zhe Dong, Xu Shen, Houqiang Li, and Xinmei Tian. 2015. Photo Quality Assessment with DCNN that Understands Image Well. In *MultiMedia Modeling. 21st International Conference, Sydney, Australia, January*. 524–535.
- [9] DPChallenge. 2017. DPChallenge. <http://www.dpchallenge.com>. (2017).
- [10] Flickr. 2017. Flickr. <http://www.flickr.com>. (2017).
- [11] Thorsten Joachims. 2006. Training linear SVMs in linear time. In *ACM SIGKDD International Conference on Knowledge Discovery and Data Mining, Philadelphia, PA, United states, August*. 217–226.
- [12] Shao Hang Kao, Wei Yen Day, and Pu Jen Cheng. 2010. An Aesthetic-Based Approach to Re-ranking Web Images. In *INFORMATION RETRIEVAL TECHNOLOGY, Taipei, Taiwan, December*. 610–623.
- [13] Yan Ke, Xiaou Tang, and Feng Jing. 2006. The Design of High-Level Features for Photo Quality Assessment. In *IEEE Computer Society Conference on Computer Vision and Pattern Recognition, New York, NY, United states, June*. 419–426.
- [14] Shu Kong, Xiaohui Shen, Zhe Lin, Radomir Mech, and Charles Fowlkes. 2016. Photo Aesthetics Ranking Network with Attributes and Content Adaptation. In *European Conference on Computer Vision*. 662–679.
- [15] Alex Krizhevsky, Ilya Sutskever, and Geoffrey E Hinton. 2012. ImageNet classification with deep convolutional neural networks. In *International Conference on*



## USAR: an interactive user-specific aesthetic ranking framework for images

- Neural Information Processing Systems, Lake Tahoe, NV, United states, December.* 1097–1105.
- [16] Kuo Yen Lo, Keng Hao Liu, and Chu Song Chen. 2012. Assessment of photo aesthetics with efficiency. In *International Conference on Pattern Recognition, Tsukuba, Japan, November*. 2186–2189.
  - [17] Kuo Yen Lo, Keng Hao Liu, and Chu Song Chen. 2012. Intelligent photographing interface with on-device aesthetic quality assessment. In *International Conference on Computer Vision, Daejeon, Korea, November*. 533–544.
  - [18] Xin Lu, Zhe Lin, Hailin Jin, Jianchao Yang, and James Z Wang. 2014. RAPID: Rating Pictorial Aesthetics using Deep Learning. In *ACM International Conference on Multimedia, Orlando, NV, United states, November, November*. 457–466.
  - [19] Yeqi Lu, Yao Shen, and Minyi Guo. 2013. Tag-based personalized image ranking in event browsing. *Peer-to-Peer Networking and Applications* 6, 4 (2013), 434–444.
  - [20] Wei Luo, Xiaogang Wang, and Xiaoou Tang. 2011. Content-based photo quality assessment. *IEEE Transactions on Multimedia* 15, 8 (2011), 1930–1943.
  - [21] Yiwen Luo and Xiaoou Tang. 2008. Photo and Video Quality Evaluation: Focusing on the Subject. In *European Conference on Computer Vision, Marseille, France, October*. 386–399.
  - [22] Hao Lv and Xinmei Tian. 2016. Learning Relative Aesthetic Quality with a Pair-wise Approach. In *MultiMedia Modeling. 22nd International Conference, Miami, FL, United states, January*. 493–504.
  - [23] Luca Marchesotti, Naila Murray, and Florent Perronnin. 2012. AVA: A Large-Scale Database for Aesthetic Visual Analysis. In *IEEE Computer Society Conference on Computer Vision and Pattern Recognition, Providence, RI, United states, June*. 2408–2415.
  - [24] Luca Marchesotti, Florent Perronnin, Diane Larlus, and Gabriela Csurka. 2011. Assessing the aesthetic quality of photographs using generic image descriptors. In *International Conference on Computer Vision, Barcelona, Spain, November*. 1784–1791.
  - [25] E. Mavridaki and V. Mezaris. 2015. A comprehensive aesthetic quality assessment method for natural images using basic rules of photography. In *IEEE International Conference on Image Processing, Quebec City, Canada, September*. 887–891.
  - [26] Naila Murray, Luca Marchesotti, and Florent Perronnin. Learning to rank images using semantic and aesthetic labels. In *PROCEEDINGS OF THE BRITISH MACHINE VISION CONFERENCE, Guildford, Surrey, United kingdom, September 3 - September 7*.
  - [27] Amandianeze O. Nwana and Tsuhan Chen. 2016. QUOTE: Querying Users as Oracles in Tag Engines a Semi-Supervised Learning Approach to Personalized Image Tagging. In *IEEE International Symposium on Multimedia, San Jose, CA, United states, December*. 30–37.
  - [28] Kayoung Park, Seunghoon Hong, Mooyeol Baek, and Bohyung Han. 2017. Personalized Image Aesthetic Quality Assessment by Joint Regression and Ranking. In *Applications of Computer Vision*. 1206–1214.
  - [29] Jian Ren, Xiaohui Shen, Zhe Lin, Radomir Mech, and David J. Foran. 2017. Personalized Image Aesthetics. In *IEEE International Conference on Computer Vision*. 638–647.
  - [30] Jitao Sang, Changsheng Xu, and Dongyuan Lu. 2011. Learn to Personalized Image Search From the Photo Sharing Websites. *IEEE Transactions on Multimedia* 14, 4 (2011), 20–21.
  - [31] Hsiao Hang Su, Tse Wei Chen, Chieh Chi Kao, Winston H. Hsu, and Shao Yi Chien. 2011. Scenic photo quality assessment with bag of aesthetics-preserving features. In *International Conference on Multimedia, Scottsdale, Az, Usa, November 28 - December 1*. 1213–1216.
  - [32] Xinmei Tian, Zhe Dong, Kuiyuan Yang, and Tao Mei. 2015. Query-Dependent Aesthetic Model With Deep Learning for Photo Quality Assessment. *IEEE Transactions on Multimedia* 17, 11 (2015), 2035–2048.
  - [33] Hanghang Tong, Mingjing Li, Hong Jiang Zhang, Jingrui He, and Changshui Zhang. 2004. Classification of Digital Photos Taken by Photographers or Home Users. In *Pacific Rim Conference on Advances in Multimedia Information Processing, Tokyo, Japan, November 30 - December 3*. 198–205.
  - [34] A. S Vijendran and C Deepa. 2014. TAD-RR: Tag-Annotation Based Demand Re-ranking Approach for Personalized Image Retrieval. In *International Conference on Intelligent Computing Applications, Coimbatore, Tamilnadu, India, March*. 440–443.
  - [35] Weining Wang, Li Wang, Mingquan Zhao, Jiacheng Cai, Tingting Shi, and Xiangmin Xu. 2016. Image Aesthetic Classification Using Parallel Deep Convolutional Neural Networks. *Acta Automatica Sinica* 42, 6 (2016), 904–914.
  - [36] Lei Yao, Poonam Suryanarayan, Mu Qiao, James Z Wang, and Jia Li. 2012. OS-CAR: On-Site Composition and Aesthetics Feedback Through Exemplars for Photographers. *International Journal of Computer Vision* 96, 3 (2012), 353–383.